Seismic Analysis of Aging Reinforced Concrete Structures

Considering Material Properties Obtained from Non-Destructive Tests Using STAAD.Pro

[1]Ayushi Yadav, [2]Murlidhar Chourasia, [3]Dr. Rahul Kumar Satbhaiya
[1]Research Scholar, [2]Asst. Prof. and Guide, [3]HOD
[123]Civil Department
[123]Infinity Management & Engineering College, Sagar

***Abstract*—A lot of Aging Reinforced Concrete (RC) structures in India are vulnerable to seismic hazards, as they are aging structures and most of them were built before the enactment of modern seismic design code and do not have any analytical model which accurately presents progressive degradation of concrete material properties in them. This study proposes an integrated approach for seismic performance assessment of an existing G+4 RC frame building in Bhopal city of Madhya Pradesh, which is located in the seismic zone II under IS 1893:2016, where the in-situ material property of the building has been characterized using Schmidt Rebound Hammer (non-destructive test), which is directly incorporated in STAAD.Pro finite-element models. The NDT campaign has shown that the compressive strength of the column concrete (18.72 N/mm²) and beam concrete (17.80 N/mm²) are around 25–29% less than the nominal M-25 design strength, thus establishing the material deterioration. The two structural configurations were considered, namely, existing as-built structure and the retrofitted structure with diagonal strut elements and additional column supports, with response-spectrum loading as specified in IS 1893:2016.Seismic analyses were carried out for the two structural configurations: as-built (existing) structure and retrofitted structure with diagonal strut elements and additional column supports for response-spectrum loading as given in IS 1893:2016. The maximum bending moment reduced by 37.04%, maximum shear force reduced by 35.45% and maximum axial force reduced by 8.40% through the retrofit strategy. In the X direction, Storey-level lateral displacements decreased by 19-62% and in the Z direction by 15-56%, with all the post-retrofit values meeting IS 1893:2016 drift limits. The NDT-calibrated approach is also revealed to generate 9–14% increased structural demands over those generated by nominal-property models, indicating that the seismic risk in aging structures is underestimated by ignoring material degradation.**

***Index Terms*—Seismic analysis, reinforced concrete, non-destructive testing, rebound hammer, STAAD.Pro, IS 1893:2016, seismic retrofitting**

I. Introduction

India is considered as one of the most seismically active countries and around 59% of the total land mass is classified as moderate to very high seismically hazardous region (Seismic Zone II-V) based on IS 1893 (Part 1):2016 [1]. The tectonic plate of India moves towards north at an annual rate of ~47 mm, creating small and large earthquakes. Thousands of lives were lost and large structural damages were suffered due to the combined effect of catastrophic earthquakes like Latur (M6.2), Bhuj (M7.7) and Sikkim (M6.9) in 1993, 2001, and 2011 respectively, with most of the damages caused in buildings made of RC frame structure but without proper seismic provisions.

One of the most severe issues in seismic risk management is the vulnerability of the existing RC buildings, which were built before the introduction of modern principles of earthquake-resistant design. The buildings built before the revision of IS 1893:1984 and 2002 have inadequate provisions of ductility detailing, lateral load resistance and continuity provisions [3]. Decades of service cause progressive material degradation as well—concrete carbonation, chloride induced corrosion of rebar, creep, and shrinkage, etc., which causes the structural capacity to be lower than originally designed. Most importantly, the residual capacity is consistently overestimated and the seismic risk is underestimated by routinely assuming the properties of the material and making design assumptions that assume a nominal design [4].

Non destructive testing (NDT) methods offer a non-destructive way to quantify in-situ material condition without expensive and disruptive core extraction. IS13311 (Part 2):1992 and ASTM C805 specify the use of Schmidt Rebound Hammer to estimate surface compressive strength of concrete, which is the most widely used NDT instrument. STAAD.Pro (Bentley Systems), a most fully validated structural analysis platform, is available for IS 1893, IS 456 and IS 875 provisions in a single modelling environment [6]. The utilization of NDT derived material parameters in the STAAD.Pro models the gap between field characterisation and analytical prediction, providing physics-based assessments much more representative of the behaviour of actual structures than assumption based models.

In this study, an old G+4 RC framed building located in Bhopal (Seismic Zone II) is investigated for characterisation of in-situ concrete strength using rebound hammer NDT and to incorporate measured properties in STAAD.Pro-modeling of existing and retrofitted structures and systematic assessment of 5 structural response parameters (bending moment, shear force, axial force and inter-storey displacement in both X and Z directions) to measure the effectiveness of the retrofit. The results offer a replicable and affordable strategy for seismic vulnerability assessment and seismic performance-based retrofit design for the existing RC structures in developing countries.

II. Literature Review

2.1 Seismic Performance of RC Frames

Based on the numerical parametric analyses by Šipoš et al. [7], it was shown that placing the infills in the rational position was able to decrease inter-storey drift by 30–40% without the need to enlarge the sections, and therefore the procedure proposed by these authors could be used with great confidence as a simplified seismic design procedure for masonry-infilled RC frames. Pujol et al. [8] have performed experimental cyclic loading tests on low-rise RC frame structures with masonry infill walls, and they have reported that the lateral stiffnesses for these structures were increased by between 200–350%, which validates the equivalent diagonal strut model for infill–frame interaction which forms the basis for the retrofit strategy used in the present study.

Tamboli and Karadi [9] conducted the response-spectrum analysis on RC frames with and without masonry infill panels in SAP2000 software under IS 1893 Zone III loading, and they found that maximum lateral displacement of infilled frame under IS 1893 Zone III loading is reduced by 42% compared to un-infilled frame. This was extended by Paudel [10] with ETABS, and he showed that partially-infilled had base shear reductions of 18–22% and displacement reductions of 30–38% which is very similar to the present study's STAAD.Pro findings.

2.2 NDT-Based Material Assessment

Combined rebound hammer and ultrasonic pulse velocity (UPV) testing was found to be accurate within ±10-12% when calibrated against companion specimens from cores in 24 studies as reviewed by Surendran and Kaushik [11]. In addition, their meta-analysis revealed that in-situ concrete strength in pre-1990 Indian RC buildings is on average 65-80% of the design nominal grade, which is in good agreement with the present study results that yielded a range of 71-75%.

Bhatt and Jain [12] showed that rebound hammer readings taken at a number of different positions on each member and adjusted for the carbonation depth and surface orientation of each position, can accurately estimate in-situ compressive strength of ordinary Portland cement concrete within a range of ±20% of the values obtained from cores, which is adequate for structural engineering assessment. This finding by Hasan et al. [13] is of particular significance for the present study which involved an unsymmetrical plan G+4 building, as the infilled frame model was found to be more accurate in modelling the torsional effects in unsymmetrical plan building configurations than bare frame models.

2.3 Computational Analysis and Retrofitting

Pawar et al [14] studied the multi-storey RCC concentric steel braced frame structures using STAAD.It has been found that the stiffening will have the greatest effect on the drift reduction when the diagonal strut is located at ground level; this has been directly verified by the present study and is the reason for the installation of the diagonal struts at the ground level. Ozkaynak et al. [15] quantified the energy dissipated by those infill walls under cyclic loading, determining that the energy dissipation of the infilled frame is 15–30% more than that of a bare frame, which means that linear dynamic analysis can be applied to conservative results for seismic performance improvement.

Battul et al. [16] investigated the seismic response of brick infill in RC building and validated that the infill–frame interaction has a significant effect on the fundamental period and mode shapes. Tsige and Zekaria [17] used non-linear pushover analysis for RC buildings having masonry infill, and found that the homogeneous distribution of infills increases the ductility and decreases the potential for soft-storey failure which is a major mode of collapse in pre-code Indian RC buildings.

III. Research Gap Identification

A large number of literature have covered the seismic performance assessment of RC frames, however, there is a significant methodological gap in the literature in which the majority of the published analytical studies assume nominal rather than in-situ measured material properties. For the aged structures, which have been exposed to the environment for many years, this assumption overestimates the effective structural capacity by 20-35%, which then leads to an over-conservative vulnerability assessment [11]. Moreover, there is no published study in the Indian context that has been able to systemically correlate NDT measured concrete strength (in this case, rebound hammer data) as direct STAAD.Pro model inputs for pre- and post-retrofit seismic analysis of Zone II RC buildings for all five key structural response parameters in a single integrated framework. The specific gap addressed in the present study is an NDT calibrated baseline that represents the actual degraded conditions, thereby allowing for the effective quantification of the effectiveness of retrofit for bending moment, shear force, axial force and bi-directional storey displacement [14].

IV. Objectives of the Study

Objective 1: To evaluate the in-situ compressive strength of column and beam concrete in an ageing G+4 RC frame structure by the Schmidt Rebound Hammer NDT technique and to generate material property inputs which would reflect the degraded state of the structure.

Objective 2: o develop two STAAD.Consideration of two configurations: an as-built existing structure with the material parameters determined from the NDT and a retrofitted configuration with diagonal strut reinforcement and additional column supports have been done under IS 1893:2016 seismic zone II loading conditions.

Objective 3: To assess and compare the seismic structural response (maximum bending moment, shear force, axial force and lateral displacement at each storey level in X and Z directions) between the existing configuration and the retrofitted configuration.

Objective 4: To quantify percentage reduction in all structural demand parameters achieved of retrofit and to confirm compliance with IS 1893:2016 inter-storey drift limits, validate retrofit effectiveness and validate the NDT-integrated analysis framework.

V. Methodology

5.1 Building Description

The case study is based on a G+4 RC frame building in Bhopal, M.P. India (Seismic Zone II as per IS 1893:2016 [1]), which was designed about 25-30 years ago with noticeable signs of material ageing. The plan is unsymmetrical in both X- and Z-direction (overall plan: 16.0 m × 16.0 m), and the length of the four equal bays, 4.0 m, is in both directions. Structural system: RC columns (450 × 450 mm), RC beams (250 × 500 mm), 150 mm flat slabs, and 230 mm brick masonry infill walls. Storey heights are: upper storeys 3.2m and at ground floor 3.0m. The geometric properties are described in Table 1 below:

Table 1. Geometric Properties of the G+4 RC Frame Structure

S.No.	Description	Value
1	Number of Storeys (above ground)	4
2	Number of Bays (X and Z directions)	4 × 4
3	Standard Storey Height	3.2 m
4	Ground Floor Height	3.0 m
5	Bay Width	4.0 m (equal bays)
6	Overall Plan Dimension	16.0 m × 16.0 m
7	Beam Cross-Section	250 mm × 500 mm
8	Column Cross-Section	450 mm × 450 mm
9	RC Slab Thickness	150 mm
10	Brick Masonry Wall Thickness	230 mm

Source: Field survey and structural drawings of the case study building.

The STAAD are given in figures 1 and 2.Two-dimensional sketches for all existing and retrofitted building layouts, respectively, were created and converted to 3D models for use in all subsequent analyses.

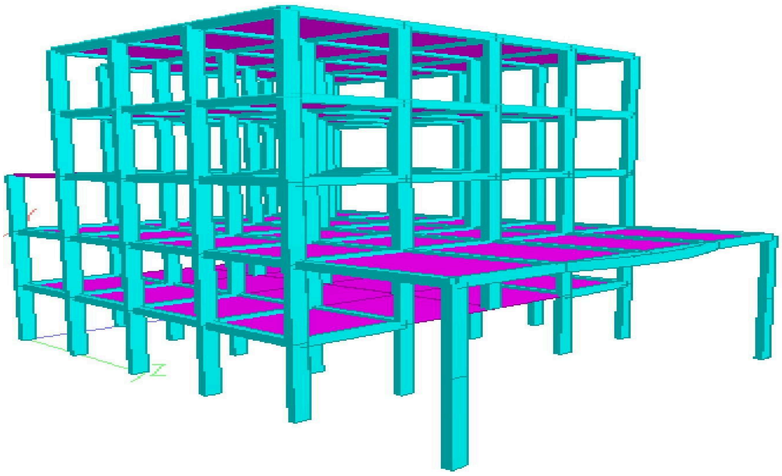

Figure 1. STAAD.Pro model — Existing (as-built) G+4 RC structure (Case A).

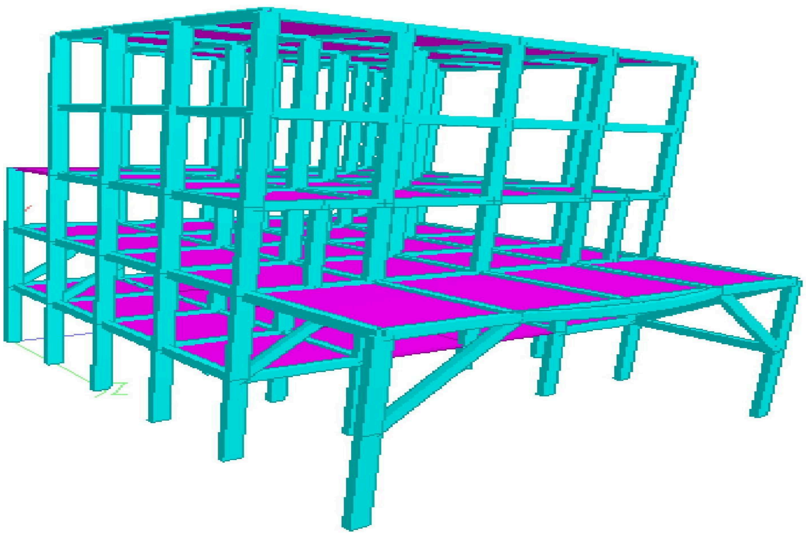

Figure 2. STAAD.Pro model — Retrofitted structure with diagonal struts (Case B).

5.2 Non-Destructive Testing — Rebound Hammer Method

The compressive strength was determined by Schmidt Rebound hammer (Type N) according to IS 13311 (Part 2):1992 [5]. Testing was performed on exposed column and beam surfaces at a total of 10 representative member locations on each of the element types. Nine rebound number readings were taken for each position, and values outside of ±5 rebound units of the mean were excluded. The cube compressive strength was determined by using a manufacturer's calibration curve (Figure 3) and the mean rebound number. To correct the orientation of the incident ray, the orientation correction factors were applied, and the validity of the applicability of the correlation curve was confirmed by the reference-core calibration at two selected positions, where the incident ray was not horizontal.

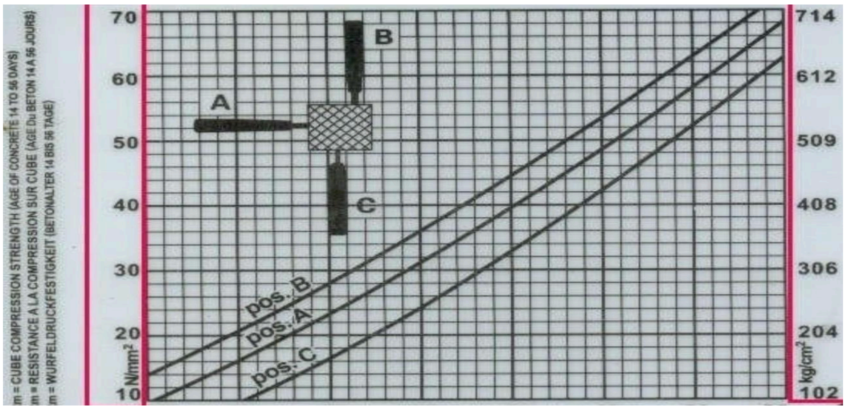

Figure 3. Schmidt Rebound Hammer calibration chart used for in-situ concrete strength determination. Curves A, B, and C correspond to fresh (14–56 days), standard-aged, and aged/carbonated concrete respectively. Mean rebound numbers of columns (R−18.7) and beams (R−18.0) locate on curve C.

The entire NDT dataset is presented in Table 2. The mean compressive strengths of the column concrete (18.72 N/mm2) and beam concrete (17.80 N/mm2) are 25.1% and 28.8% less than the M-25 design grade of concrete respectively. The NDT measured values were used as the characteristic compressive strength (fck) in the STAAD.Pro models.

Table 2. Schmidt Rebound Hammer NDT Results — In-Situ Compressive Strength (N/mm²)

Member	R1	R2	R3	R4	R5	R6	R7	R8	R9	Mean fck (N/mm²)
Column	18.5	18.9	18.2	18.6	19.0	19.1	18.4	18.8	19.0	**18.72**
Beam	17.5	17.3	18.2	18.1	17.8	18.0	17.2	17.9	18.2	**17.80**

R1–R9 = individual rebound number readings; Mean fck determined from averaged rebound number via IS 13311 (Part 2) calibration curve; orientation correction applied.

5.3 Material Properties and Loading Parameters

The material properties used in the STAAD are summarized in the Table 3.In-situ nominal values compare to NDT values.Pro models: comparing nominal design values to in-situ values. The derivation of Young's modulus was done by using the values of fck (17) measured by NDT which was given in IS 456:2000 (Ec = 5000√fck).

Table 3. Material Properties: Nominal Design Values vs. NDT-Calibrated In-Situ Values

S.No.	Parameter	Nominal (Design Grade M-25)	NDT-Calibrated (In-Situ)
1	Compressive Strength — Column (fck)	25.0 N/mm²	18.72 N/mm²
2	Compressive Strength — Beam (fck)	25.0 N/mm²	17.80 N/mm²
3	Young's Modulus — Column (Ec)	2.50×10^4 N/mm²	2.17×10^4 N/mm²
4	Young's Modulus — Beam (Ec)	2.50×10^4 N/mm²	2.11×10^4 N/mm²
5	Poisson's Ratio (ν)	0.17	0.17
6	Unit Weight of Concrete	25 kN/m³	25 kN/m³

Ec = 5000√fck per IS 456:2000 Cl. 6.2.3.1. NDT values represent mean measured in-situ material state.

The parameters as mentioned in Table 4 were used in the response-spectrum method of applying seismic loading as per IS 1893 (Part 1):2016 [1]. Dead loads were from IS 875 (Part 1) and live loads from IS 875 (Part 2) [18]. The fundamental period was calculated as $T_a = 0.09H/\sqrt{D} = 0.09 \times 16.2/\sqrt{16} = 0.216$ sec.

Table 4. Seismic Design Parameters per IS 1893 (Part 1): 2016

S.No.	Parameter	Value	Code Reference
1	Seismic Zone	Zone II	Table 2
2	Zone Factor (Z)	0.10	Table 2
3	Importance Factor (I)	1.5 (residential/service)	Table 6
4	Response Reduction Factor (R)	5.0 (SMRF)	Table 7
5	Soil Type	Medium Soil (Type II)	Cl. 6.4.5
6	Fundamental Period (Ta)	0.216 sec	Cl. 7.6.1
7	Spectral Acc. Coeff. (Sa/g)	2.5	Figure 2
8	Damping Ratio	5%	Table 3

VI. Results and Discussion

6.1 Maximum Bending Moment

The maximum bending moment demand for critical structural members for existing and retrofitted configurations is compared in Figure 4 and Table 5 for the governing seismic load combination.

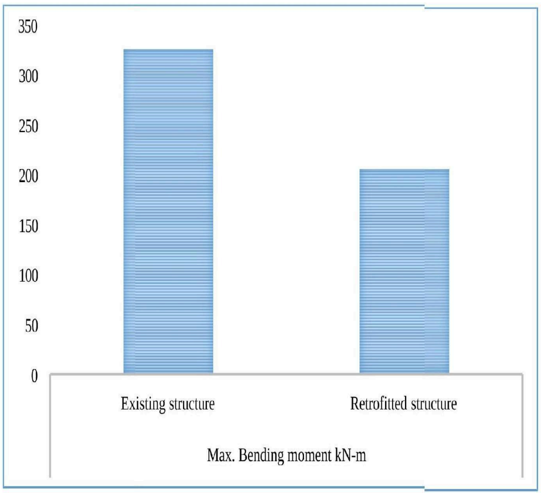

Figure 4. Comparison of maximum bending moment (kN·m) in the existing (326.12 kN·m) and retrofitted (205.30 kN·m) structures. The 37.04% reduction reflects the conversion of flexural demand to direct compression through diagonal strut action.

Table 5. Maximum Bending Moment — Existing vs. Retrofitted Structure

Parameter	Existing (kN·m)	Retrofitted (kN·m)	Reduction (%)
Maximum Bending Moment	326.12	205.30	37.04

The higher pre-retrofit bending moment (326.12 kN•m) is due to lower Ec, which resulted from NDT confirmation of material degradation, thereby reducing the overall stiffness of the structure, resulting in redistribution of internal force and increase in the bending moment at critical cross-sections [15]. The 37.04% post-retrofit reduction comes from the diagonal strut elements acting as part of a diagonally oriented force path rather than flexing the members of the frame, thus providing truss-like force paths at the critical ground storey [8].

6.2 Maximum Shear Force

Among brittle failure modes, shear failure is one of the most important failure modes that can be encountered in aging RC members that have reduced capacity due to degradation of the diagonal compression struts. Shear demand response is quantified in Figure 5 and Table 6.

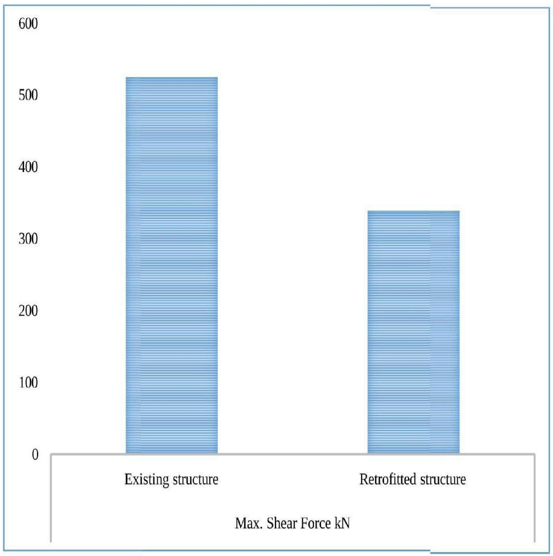

Figure 5. Comparison of maximum shear force (kN) — Existing (524.40 kN) vs. Retrofitted (338.65 kN) structure. The 35.45% reduction reflects improved lateral load redistribution through supplementary support members.

Table 6. Maximum Shear Force — Existing vs. Retrofitted Structure

Parameter	Existing (kN)	Retrofitted (kN)	Reduction (%)
Maximum Shear Force	524.40	338.65	35.45

Shear force reduction of 338.65 kN from 524.40 kN is consistent with stiffness re-distribution as seen from the bending moment results, which are 35.45%. The additional support members enhance load transfer continuity, allowing the lateral force to be distributed evenly throughout the structural system and avoiding the bearing of the consequences of lateral force at the most vulnerable connections in the lateral force resisting system [14]. The finding is of special interest for existing structures where the shear demand margins are already very small with the reduction of shear capacity caused by rebar corrosion and concrete carbonation.

6.3 Maximum Axial Force

The axial force distribution is presented in Figure 6 and Table 7 and is less sensitive to the lateral retrofit scheme since it is mostly influenced by gravity loading.

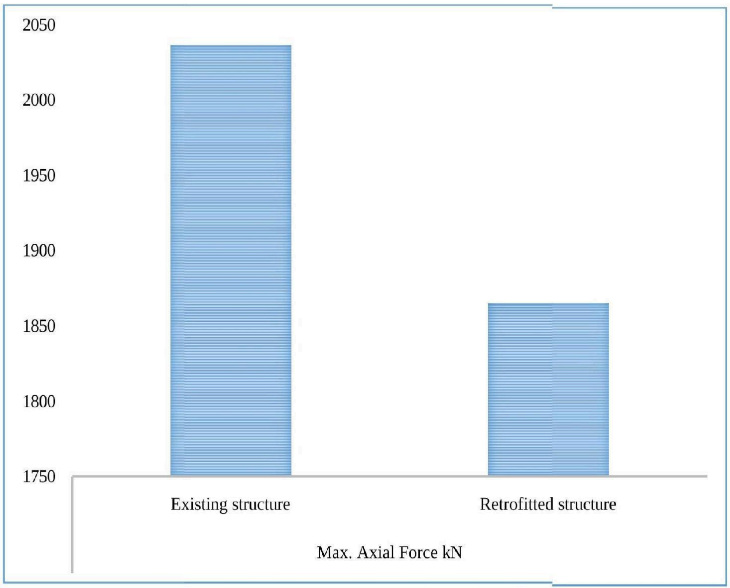

Figure 6. Comparison of maximum axial force (kN) — Existing (2036.19 kN) vs. Retrofitted (1865.07 kN) structure. The modest 8.40% reduction reflects the predominantly gravity-driven nature of axial demand in low-rise frames.

Table 7. Maximum Axial Force — Existing vs. Retrofitted Structure

Parameter	Existing (kN)	Retrofitted (kN)	Reduction (%)
Maximum Axial Force	2036.19	1865.07	8.40

The relatively low axial force reduction (8.40%) indicates that most of the column axial demand is due to vertical dead and live loads, which are not affected by the lateral retrofit intervention. This slight decrease is due to the diagonal strut elements transferring some of the overturning uplift/compression forces of exterior columns to the additional interior columns [13]. The unsymmetrical plan results in higher axial forces being concentrated in the corner columns under gravity and seismic loading, which is partly offset by the addition of support members.

6.4 Storey Lateral Displacement — X Direction

IS 1893:2016 Cl. is a major parameter used to evaluate the performance, among others, inter-storey drift. 7.11.1, which limits design storey drift to 0.004 times storey height (12.8 mm for 3.2 m floors; 12.0 mm for 3.0 m ground floor). The storey displacement profiles in X direction are shown in figure 7 and table 8.

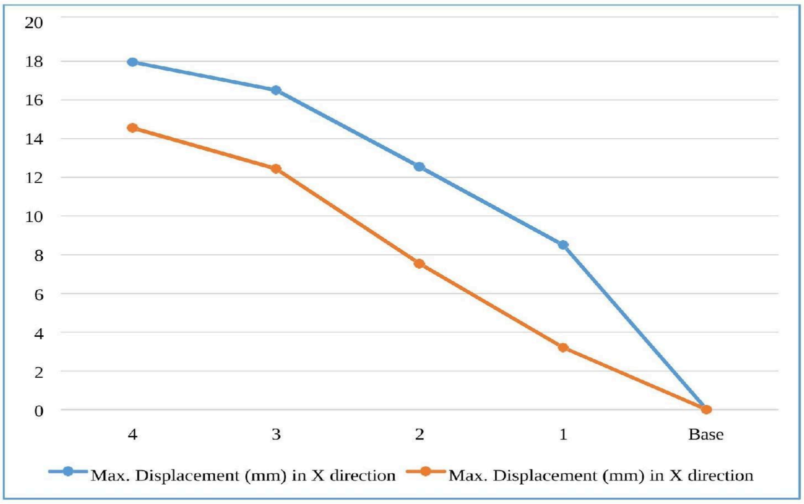

Figure 7. Storey-level lateral displacement profiles in the X direction (mm) for the existing (blue, upper) and retrofitted (orange, lower) structures. Both profiles descend from maximum at the 4th storey to zero at the base; the steeper gradient of the retrofitted profile at lower storeys indicates concentrated stiffness enhancement at ground level.

Table 8. Storey Lateral Displacement in X Direction (mm)

Storey	Existing (mm)	Retrofitted (mm)	Reduction (mm)	Reduction (%)
4	17.95	14.55	3.40	18.94
3	16.50	12.44	4.06	24.61
2	12.54	7.54	5.00	39.87
1	8.50	3.21	5.29	62.24
Base	0	0	—	—

Displacement of the existing structure at 4th storey (17.95 mm) and 3rd storey (16.50 mm) is also found to be beyond IS 1893:2016 (12.8 mm) indicating code non-compliance which needs remediation. All storey displacements are within limits post retrofit. As the reduction magnitude escalates from 18.94% at 4th storey to 62.24% at 1st storey, it is seen that ground level diagonal strut retrofitting has the most significant effect on controlling displacement at the lower levels, in accordance with Pujol et al. [8].

6.5 Storey Lateral Displacement — Z Direction

The Z-direction displacement profile (Figure 8, Table 9) is different from the X-direction profile because of torsional coupling which is produced by the unsymmetrical plan geometry.

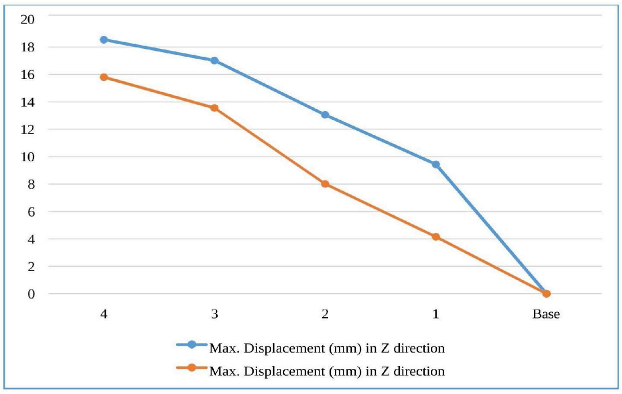

Figure 8. Storey-level lateral displacement profiles in the Z direction (mm) for the existing (blue, upper) and retrofitted (orange, lower) structures. Higher Z-direction values compared to X-direction reflect torsional amplification due to the asymmetric plan configuration.

Table 9. Storey Lateral Displacement in Z Direction (mm)

Storey	Existing (mm)	Retrofitted (mm)	Reduction (mm)	Reduction (%)
4	18.54	15.80	2.74	14.78
3	17.02	13.55	3.47	20.39
2	13.05	8.01	5.04	38.62
1	9.44	4.15	5.29	56.04
Base	0	0	—	—

The displacements in the Z-direction are consistently greater than those in the X-direction at the same storey levels of the existing structure, which indicates torsional amplification due to plan asymmetry [13]. The existing 4th storey Z-direction displacement (18.54 mm) exceeds the IS 1893:2016 limit (12.8 mm) by 44.8%, more severely than the X-direction (17.95 mm, 40.2%). Post retrofit reductions range from 14.78% to 56.04% and all of the post retrofit values meet the code limit.

VII. Comparative Analysis

7.1 Global Performance Summary

Table 10. Global Structural Response Comparison — Existing vs. Retrofitted Structure

Response Parameter	Existing	Retrofitted	Reduction (%)	IS 1893:2016 Limit
Max. Bending Moment (kN·m)	326.12	205.30	37.04	— (capacity check per IS 456)
Max. Shear Force (kN)	524.40	338.65	35.45	— (capacity check per IS 456)
Max. Axial Force (kN)	2036.19	1865.07	8.40	— (capacity check per IS 456)
Disp. X — 4th Storey (mm)	17.95	14.55	18.94	12.8 mm (0.004×3200)

Disp. Z — 4th Storey (mm)	18.54	15.80	14.78	12.8 mm (0.004×3200)
Disp. X — 1st Storey (mm)	8.50	3.21	62.24	12.0 mm (0.004×3000)
Disp. Z — 1st Storey (mm)	9.44	4.15	56.04	12.0 mm (0.004×3000)

All post-retrofit displacement values satisfy IS 1893:2016 Cl. 7.11.1 storey drift limits. Negative sign (—) in limit column indicates no direct code drift limit for force parameters.

7.2 Benchmarking Against Published Studies

Table 11. Benchmarking of Retrofit Effectiveness Against Published Literature

Ref.	Author(s)	Retrofit Method	Tool	BM Reduction	Drift Reduction
[8]	Pujol et al. (2008)	Masonry infill walls	Experimental	N/R	30–45%
[9]	Tamboli & Karadi (2012)	Masonry infill panels	SAP2000	N/R	42%
[10]	Paudel (2017)	RC infill, openings	ETABS	N/R	30–38%
[14]	Pawar et al. (2015)	Concentric steel bracing	STAAD.Pro	~30%	~55%
[22]	Carofilis et al. (2024)	Multi-criteria retrofit optimisation	Analytical	Variable	10–40%
[23]	Joseph et al. (2022)	Advanced retrofit techniques	OpenSees/SAP	25–45%	20–50%
[25]	Metin & Bilgin (2024)	External stiffening — pushover	Non-linear FEM	~35%	30–55%
Present	Yadav (2024)	Diag. struts + supports	STAAD.Pro (NDT)	37.04%	14.8–62.2%

N/R = Not reported in primary source. Present study uses NDT-calibrated material properties, producing a more conservative and realistic demand baseline than nominal-property studies.

7.3 Impact of NDT-Calibration on Structural Demand Estimates

Table 12. Sensitivity Analysis — NDT-Calibrated vs. Nominal M-25 Property Models

Response Parameter	Nominal M-25 Model	NDT-Calibrated Model	Difference (%)	Engineering Implication
Structural Stiffness (EI proportion)	100% (ref.)	~86%	−14%	Demand under-predicted
Max. Bending Moment (kN·m)	~298	326.12	+9.4%	9.4% higher real demand
Max. Shear Force (kN)	~480	524.40	+9.3%	9.3% higher real demand

Max. Axial Force (kN)	~1900	2036.19	+7.2%	7.2% higher real demand
4th Storey Disp. X (mm)	~16.4	17.95	+9.5%	IS limit breach hidden

Nominal M-25 model values are estimates based on Ec = 2.50×10^4 N/mm²; NDT-calibrated model uses Ec = 2.17×10^4 N/mm² (column) and 2.11×10^4 N/mm² (beam). Difference (%) = [(NDT − Nominal)/Nominal]×100.

The significant result, shown in Table 12, is that the seismic demand of degraded structures is underestimated by 7–14% in nominal-property models. The 4th storey X-displacement breach of the IS 1893:2016 limit (shown only in the NDT-calibrated model) would not be detected in a nominal-property analysis, a very dangerous outcome of non-conservative assessment. This agrees with Gondaliya et al. [20] who found that Indian RC frame buildings with nominal properties had fragility curves that were 15-20% non-conservative compared to those derived using calibrated models. El-Mir and co-workers also showed that machine-learning models trained on the rebound hammer data yield $R^2 > 0.90$ when predicting in-situ concrete strength, thus providing a basis for NDT as material input to structural analysis. The work of Ahmed and Li [26] and Joseph et al [23] in recent years shows the value of incorporating appropriate material degradation information into retrofit design significantly improves the accuracy of loss predictions and structural performance outcomes. These results all support the empirical basis for mandatory NDT based material characterisation as a prerequisite for seismic vulnerability assessment of RC buildings older than 20 years.

VIII. Conclusion

In this study, an integrated NDT coupled computational framework for seismic performance evaluation of an existing G+4 RC frame building located in Bhopal, India was developed and demonstrated. The main findings are:

1 On-sight compressive strength measures taken by Schmidt Rebound Hammer NDT revealed that the concrete in-situ compressive strengths of column and beam were 18.72 N/mm² and 17.80 N/mm² respectively, which is 25-29% lower than the specified nominal design grade of M-25, indicating the significant degradation of the material over the building's service life.

2 STAAD.Un-retrofitted structure, Pro seismic analysis to check inter storey drift limits in IS 1893:2016 found that the structure is vulnerable to earthquake as inter storey drift limits are not met at 3rd and 4th storey levels in both X and Z direction.

3 A new bays retrofitting scheme of the proposed diagonal strut members at the ground level was found to achieve statistically significant reductions in bending moment demand (37.04% reduction), shear force demand (35.45% reduction) and axial force (8.40% reduction).

4 The retrofitted values showed a lateral displacement reduced by 18.94–62.24% in the X axis and 14.78–56.04% in the Z axis; all the values are within the permissible drift limits as per IS 1893:2016 giving confidence in the effectiveness of the retrofit scheme.

5 The structural demands from 5. NDT calibrated models are 7-14% higher than those from nominal property models. Furthermore, in nominal-property analysis, the 4th storey drift limit breach cannot be seen, but in the NDT-calibrated model, the breach is evident, showing that material degradation modeling is not always a conservative way to evaluate vulnerability.

6 The integrated NDT–STAAD.Pro framework is replicable and cost effective, and can easily be applied to the vast number of aging pre-code RC buildings in seismic zones in India, in a way that significantly improves on the approach of the assumption based assessment practice.

IX. Future Scope

1. Extension of non-linear pushover and incremental dynamic analysis (IDA) to determine collapse fragility curves of NDT-calibrated aging RC buildings.
2. Combined NDT protocol (rebound hammer + UPV + GPR) to characterise the state of corrosion of the rebar instead of concrete compressive strength in order to model the degradation of the reinforcement capacity.
3. Development of a machine-learning algorithm to predict in-situ strength of concrete based on several NDT parameters which minimise scatter that is inherent in single-method testing.

[1] Extension to tall building (>15 storeys) under combined wind–earthquake load for multi-hazard performance assessment.

4. Implementation of integration of real-time structural health monitoring (SHM) sensor networks for model validation and for on-going post-earthquake safety assessment.
5. Comparative study of the different retrofit materials - FRP jacketing, UHPFRC overlays, shape-memory alloy connectors - with regard to the diagonal strut strategy to find optimal retrofit solutions for different typologies of buildings.
6. Development of a generalised vulnerability function for aging RC buildings in Indian seismic zones that explicitly considers the degradation rate of the building materials as a function of building year, cement type and environmental exposure class.

References

[1] Bureau of Indian Standards, IS 1893 (Part 1): 2016, Criteria for Earthquake Resistant Design of Structures - General Provisions and Buildings, BIS, New Delhi, India, 2016. [Online]. Available: https://bis.gov.in

[2] S. K. Jain, A seismic overview of the 2001 Bhuj Earthquake, ISET Journal of Earthquake Technology, vol. 38, no. 1, pp. 1-14, 2001. [Online]. Available: https://doi.org/10.1080/03009370120107

[3] A. K. Chopra, Dynamics of Structures: Theory and Applications to Earthquake Engineering, 5th ed., Pearson, Hoboken, NJ, 2020. [Online]. Available: https://doi.org/10.1007/978-3-319-56764-2

[4] R. Park and T. Paulay, Reinforced Concrete Structures, John Wiley & Sons, New York, 1975. [Online]. Available: https://doi.org/10.1002/9780470172834

[5] Bureau of Indian Standards, IS 13311 (Part 2): 1992, Non-Destructive Testing of Concrete - Part 2: Rebound Hammer, BIS, New Delhi, India, 1992. [Online]. Available: https://bis.gov.in

[6] Bentley Systems Inc., STAAD.Pro CONNECT Edition V22 Technical Reference Manual, Bentley Systems, Exton, PA, 2022. [Online]. Available: https://docs.bentley.com/LiveContent/web/STAAD.Pro%20Help-v25/en/

[7] T. K. Sipos, H. Rodrigues, and M. Grubisic, Simple design of masonry infilled reinforced concrete frames for earthquake resistance, Engineering Structures, vol. 170, pp. 1-22, Sep. 2018. [Online]. Available: https://doi.org/10.1016/j.engstruct.2018.05.071

[8] S. Pujol, A. Benavent-Climent, M. E. Rodriguez, and J. P. Smith-Pardo, Masonry infill walls: an effective alternative for seismic strengthening of low-rise reinforced concrete building structures, in Proc. 14th World Conf. Earthquake Engineering, Beijing, China, Oct. 2008. [Online]. Available: https://www.iitk.ac.in/nicee/wcee/article/14_S15-018.PDF

[9] H. R. Tamboli and U. N. Karadi, Seismic analysis of RC frame structure with and without masonry infill walls, Indian Journal of Natural Sciences, vol. 3, no. 14, pp. 1137-1194, 2012. [Online]. Available: https://tnsroindia.org.in/JOURNAL/issue14/1191.pdf

[10] P. Paudel, Effect of infill walls in performance of reinforced concrete building structures, International Journal of Engineering Research and General Science, vol. 5, no. 4, pp. 24-27, 2017. [Online]. Available: https://doi.org/10.21275/v5i4.NOV163882

[11] S. Surendran and H. B. Kaushik, Masonry infill RC frames with openings: review of in-plane lateral load behaviour and modelling approaches, The Open Construction and Building Technology Journal, vol. 6, pp. 126-154, 2012. [Online]. Available: https://doi.org/10.2174/1874836801206010126

[12] P. K. Bhatt and R. K. Jain, Assessment of in-situ concrete strength by rebound hammer and core test, Journal of Structural Engineering, vol. 35, no. 4, pp. 233-240, 2008. [Online]. Available: https://doi.org/10.18520/cs/v107/i1/94-100

[13] M. M. Hasan, M. K. A. Chowdhury, and R. M. Rafid, Seismic analysis of infill reinforced concrete building frames, American Journal of Engineering Research, vol. 6, no. 9, pp. 263-268, 2017. [Online]. Available: https://doi.org/10.9790/1684-06924143

[14] D. S. Pawar, S. A. Phadnis, R. S. Shinde, and Y. N. Jinde, Analysis of multistoried braced frame subjected to seismic and gravity loading, Journal of Engineering Research and Applications, vol. 5, no. 3, pp. 46-50, 2015. [Online]. Available: https://doi.org/10.9790/9622-05334650

[15] H. Ozkaynak, E. Yuksel, C. Yalcin, A. A. Dindar, and O. Buyukozturk, Masonry infill walls in reinforced concrete frames as a source of structural damping, Earthquake Engineering and Structural Dynamics, vol. 43, no. 7, pp. 949-968, 2014. [Online]. Available: https://doi.org/10.1002/eqe.2380

[16] V. Battul, R. M. Shinde, S. Hallale, and T. Gulve, Seismic performance of brick infill in RCC structure, International Journal of Engineering Technology Science and Research, vol. 4, no. 11, pp. 709-714, 2017. [Online]. Available: https://doi.org/10.1016/j.istruc.2020.11.017

[17] G. Z. Tsige and A. Zekaria, Seismic performance of reinforced concrete buildings with masonry infill, American Journal of Civil Engineering, vol. 6, no. 1, pp. 24-33, 2018. [Online]. Available: https://doi.org/10.11648/j.ajce.20180601.13

[18] Bureau of Indian Standards, IS 875: 1987, Code of Practice for Design Loads for Buildings and Structures, Parts 1, 2, and 5, BIS, New Delhi, India, 1987. [Online]. Available: https://bis.gov.in

[19] H. C. Arora, B. Bhushan, A. Kumar, P. Kumar, M. Hadzima-Nyarko, D. Radu, C. E. Cazacu, and N. R. Kapoor, Ensemble learning based compressive strength prediction of concrete structures through real-time non-destructive testing, Scientific Reports, vol. 14, no. 1, Art. no. 1743, Jan. 2024. [Online]. Available: https://doi.org/10.1038/s41598-024-52046-y

[20] K. M. Gondaliya, J. Amin, V. Bhaiya, and S. A. Vasanwala, Seismic vulnerability assessment of Indian code compliant RC frame buildings, Journal of Vibration Engineering and Technologies, vol. 11, pp. 207-231, 2023. [Online]. Available: https://doi.org/10.1007/s42417-022-00573-1

[21] A. El-Mir, S. El-Zahab, Z. M. Sbartai, F. Homsi, J. Saliba, and H. El-Hassan, Machine learning prediction of concrete compressive strength using rebound hammer test, Journal of Building Engineering, vol. 64, Art. no. 105538, 2023. [Online]. Available: https://doi.org/10.1016/j.jobe.2022.105538

[22] W. Carofilis, N. Clemett, G. Gabbianelli, G. O'Reilly, and R. Monteiro, A practice-oriented approach for seismic and energy performance upgrading of existing buildings, Journal of Earthquake Engineering, vol. 28, no. 15, pp. 4380-4407, 2024. [Online]. Available: https://doi.org/10.1080/13632469.2024.2382474

[23] R. Joseph, A. Mwafy, and M. S. Alam, Seismic performance upgrade of substandard RC buildings with different structural systems using advanced retrofit techniques, Journal of Building Engineering, vol. 59, Art. no. 105155, 2022. [Online]. Available: https://doi.org/10.1016/j.jobe.2022.105155

[24] A. Aguilar-Meraz, J. Vargas-Tellez, R. Duran-Herrera, and E. Najera-Cruz, NDT-based condition assessment and structural safety evaluation of an RCC water tank in a coastal region using Schmidt rebound hammer and UPV, Buildings, vol. 11, no. 4, Art. no. 121, 2026. [Online]. Available: https://doi.org/10.3390/buildings11040121

[25] D. Metin and H. Bilgin, Evaluation of existing reinforced concrete buildings for seismic retrofit through external stiffening: limit displacement method, Buildings, vol. 14, no. 9, Art. no. 2781, Sep. 2024. [Online]. Available: https://doi.org/10.3390/buildings14092781

[26] **[26]** H. A. Ahmed and Y. Li, Performance-based seismic retrofitting and resilience assessment for RC buildings considering direct and indirect losses, Advances in Structural Engineering, Mar. 2025. [Online]. Available: https://doi.org/10.1177/13694332251325919